Sensitivity of Hot Film Flow Meter in Four Stroke Gasoline Engine

Gangyoung Lee, Cha-Lee Myung, Simsoo Park*
Department of Mechanical Engineering, Korea University,
1, 5-Ka, Anam-Dong, Sungbuk-Ku, Seoul 136-701, Korea
Youngjin Cho
Daewoo Heavy Industries & Machinery LTD

The air fuel ratios of current gasoline engines are almost controlled by several air flow meters. When CVVT (Continuous Variable Valve Timing) is applied to a gasoline engine for higher engine performance, the MAP (Manifold Absolute Pressure) sensor is difficult to follow the instantaneous air fuel ratio due to the valve timing effect. Therefore, a HFM (Hot Film Flow Meter) is widely used for measuring intake air flow in this case. However, the HFMs are incapable of indicating to reverse flow, the oscillation of intake air flow has an negative effect on the precision of the HFM. Consequently, the various duct configurations in front of the air flow sensor affect the precision of HFM sensitivity. This paper mainly focused on the analysis of the reverse flow, flow fluctuation in throttle upstream and the geometry of intake system which influence the HFM measurement.

Key Words : HFM (Hot Film Flow Meter), Reverse Flow, Flow Oscillation, CVVT (Continuous Variable Valve Timing), MAP (Manifold Absolute Pressure), USFM (Ultra Sonic Flow Meter), Intake Air Duct

Nomenclature

ABDC : After Bottom Dead Center (degree)
ATDC : After Top Dead Center (degree)
BBDC : Before Bottom Dead Center (degree)
BTDC : Before Top Dead Center (degree)
CA   : Crank Angle (degree)
CVVT : Continuous Variable Valve Timing
MAP : Manifold Absolute Pressure
HFM : Hot Film Flow Meter
rpm : Revolution Per Minute
USFM : Ultra Sonic Flow Meter
WOT : Wide Open Throttle
$a_{0,T}$: Non flow sonic velocity when air temperature is $T(K)$ (m/s)

k : Specific heat ratio of air
R : Gas constant
L_s : Length from ultra sonic receiver to transmitter in ultra sonic flow meter (m)
u : Flow velocity (m/s)
θ : Ultra sonic wave angle between receiver and transmitter

* Corresponding Author,
  E-mail : spark@korea.ac.kr
  TEL : +82-2-3290-3368; **FAX :** +82-2-926-9290
  Department of Mechanical Engineering, Korea University, 1, 5-Ka, Anam-Dong, Sungbuk-Ku, Seoul 136-701, Korea. (Manuscript **Received** April 3, 2003; **Revised** December 9, 2003)

1. Introduction

The methods for reducing engine-out exhaust emissions are improvement of the engine hardware, electronic control and after treatment appliances. In electronic control, it is well known that air flow meter and oxygen sensor play an important role in feed-back control of air fuel ratio.

Air flow meters are classified by speed density type using MAP (Manifold Absolute Pressure) sensor and direct method using an air mass flow sensor. The speed density type calculates air mass

flow indirectly by measuring absolute pressure in the intake manifold, while the HFM (Hot Film Flow Meter) eliminates the calculation of air. The speed density method has problems such as the possibility of a vacuum leak and non-detecting water vapor. Especially, the VVT (Variable Valve Timing) is applied for higher engine performance, the effect of intake valve motion gives a negative effect on air flow measurement by MAP sensor. Therefore the HFM is widely adopted for precise measurement of air mass flow (Hendricks, 1990 ; Heywood, 1988).

Though HFM has advantage over MAP sensor, flow fluctuation and reverse flow aggravate the precision of the HFM. To overcome above problems, sensor makers suggest enough length in front of the HFM and inserted duct in the air cleaner. And air mass flow rate has different value at HFM location because of various air flow profiles at cross sections of the duct. (Svoboda, 2000 ; Ohata 1982 ; Sumal, 1984).

In this research, the reverse flow, flow fluctuation and the geometry of intake system are investigated to improve the sensitivity of HFM.

2. Experimental Methods

Figure 1 shows the schematic diagram of experimental apparatus. The HFM is installed at the air duct in front of the surge tank. The USFM (Ultra Sonic Flow Meter) is used for measurement of flow direction and air mass flow at the upstream of the HFM. The laminar flow meter and the air damper (300l) are installed for more precise air flow measurement.
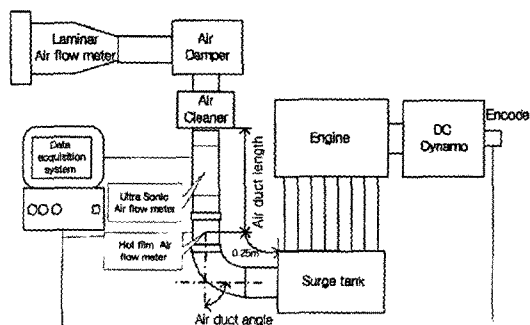
Table 1 shows the engine specifications. The DC dynamometer is used for the engine operation. The encoder is attached to the DC dynamometer and the trigger signal from encoder is coincided with the TDC (Top Dead Center) of the engine to determine every CA (Crank Angle). The M8 (MoTec Company) engine controller is used to control fuel injection time, injection duration and spark timing.

The USFM has no influence on the intake air flow because of non contact device. Figure 2 shows the schematic diagram of a transit time type USFM. The USFM theory is as follows (Hwang, 1997). The ultra sonic sender and receiver are respectively installed in forward and backward direction. The ultra sonic sender 1 and 2 generate the same phase ultra sonic wave at the same time. In the case of forward flow, sonic transmission velocity increases by flow velocity. Therefore $a_{0,T}$ becomes $a_{0,T}+\dfrac{k+1}{2} u \cos \theta$. The elapsed time when sonic wave reaches L_s (length from sender

Table 1 Specifications of test engine

Engine type	In line, DOHC, 16 Valve
Bore (mm)	85
stroke (mm)	88
Number of cylinder	4
Displacement (cc)	1996
Compression ratio	10.0 : 1
Fuel management system	MPI
Valve timing	IVO : 8° BTDC IVC : 40° ABDC EVO : 50° BBDC EVC : 10° ATDC

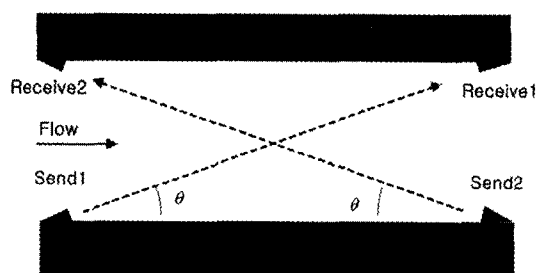**Fig. 1** Schematic diagram of experimental apparatus

Fig. 2 Schematic diagram of transit time type Ultra Sonic Flow Meter

to receiver) is the time t_1 of Eq. (1). However, in the case of backward air flow, flow direction and sonic transmission direction are opposite; hence sonic transmission velocity decreases from $a_{0,T}$ to $a_{0,T} - \dfrac{k+1}{2} u \cos\theta$ so the transmission time t_2 becomes Eq. (2). If air does not flow, $t_1 = t_2$. However if air flows in forward direction, t_2 is greater than t_1.

$$t_1 = \frac{L_s}{a_{0,T} + \dfrac{k+1}{2} u \cos\theta} \tag{1}$$

$$t_2 = \frac{L_s}{a_{0,T} - \dfrac{k+1}{2} u \cos\theta} \tag{2}$$

From Eq. (1) and (2), the transmission time difference t_d can be expressed as Eq. (3).

$$t_d = \frac{(k+1) L_s u \cos\theta}{a^2_{0,T} - \left(\dfrac{k+1}{2}\right)^2 u^2 \cos^2\theta} \tag{3}$$

u (air flow velocity) can be calculated from t_d. However, because it is difficult to make electric circuits simple, Eq. (3) must be linearized using Taylor series.

$$t_d = \frac{(k+1) L_s u \cos\theta}{a^2_{0,T} - \left(\dfrac{k+1}{2}\right)^2 u^2 \cos^2\theta}$$

$$= \frac{(k+1) L_s u \cos\theta}{a^2_{0,T}} \left(1 + \frac{\left(\dfrac{k+1}{2} u \cos\theta\right)^2}{a^2_{0,T}}\right) \tag{4}$$

In this study, u is relatively small value compared to $a_{0,T}$, $\dfrac{u^2}{a^2_{0,T}} \ll 1$, so this term is negligible. For that reason, Eq. (4) can be linearized as Eq. (5). Assuming that air is the ideal gas, non flow sonic velocity becomes $a_{0,T} = \sqrt{kRt}$ then Eq. (5) is written as Eq. (6).

$$t_d = \frac{(k+1) L_s u \cos\theta}{a^2_{0,T}} \tag{5}$$

$$u = \frac{kRT}{(k+1) L_s \cos\theta} t_d \tag{6}$$

Air flow velocity is the function of air temperature and travelling time difference of sonic wave. From Eq. (6), u is calculated by t_d. When the reverse flow occurs, t_d has negative value; thus air flow magnitude is determined.

The USFM generates voltage output signal with various air flow velocities and this signal is calibrated by the laminar flow meter. Eq. (7) represents the relationship between USFM output voltage and air mass flow.

$$\begin{aligned}&Air \ mass \ flow\\ &= 0.2698 + 14.143 * USFM \ (Voltage)\end{aligned} \tag{7}$$

3. Experimental Results

3.1 Air mass flow according to the throttle opening rate

In this study, the air flow pattern in throttle upstream is investigated at practical engine operating condition (700~2400 rpm).

Figure 3 shows the air mass flow with throttle opening rate at motoring condition. As throttle opening angle reaches at certain value, air mass flow is saturated. Air mass flow is early saturated at low engine speed and low throttle opening rate. The reverse flow occurs in the saturation region because the surge tank pressure approaches to ambient pressure.

3.2 Air mass flow in throttle upstream

Figure 4 shows the averaged and instantaneous air mass flow at 800 rpm, WOT condition. As the HFM has insensitivity to opposite flow, reverse flow can be quantified with USFM. The HFM detects the reverse flow as forward flow, so the flow pattern of HFM shows higher flow rate. The averaged air mass flow by HFM is 24.6(g/s)
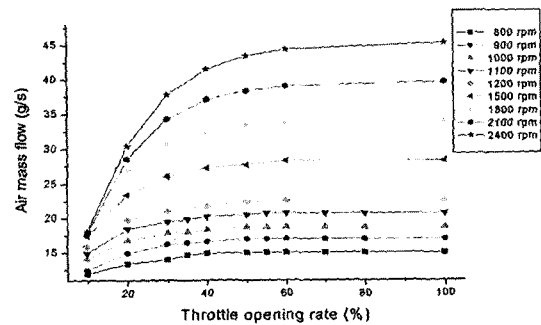

Fig. 3 Air mass flow vs. throttle opening rate

while that by USFM is 17.3(g/s).

Figure 5 represents the air mass flow at 1200 rpm, WOT condition. In spite of without reverse flow, the HFM has 2% errors which is caused by HFM's slow response time. The measurement error of HFM is summarized as follows. 1) insensitivity to opposite flow, 2) slow response time.
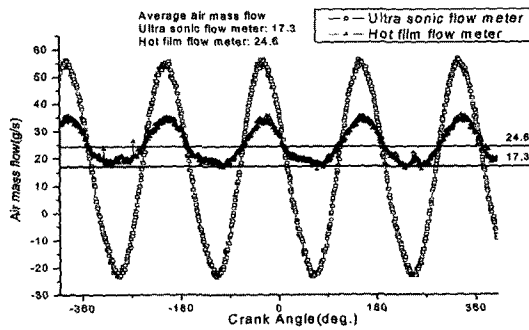
Figure 6 shows the air mass flow measured

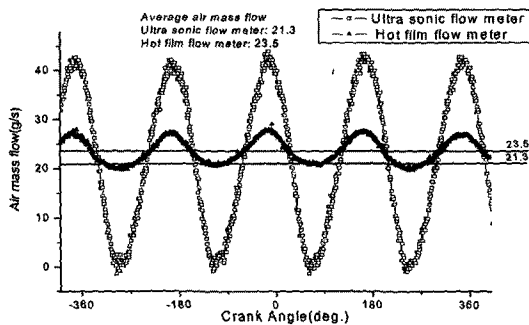**Fig. 4** Comparison of air mass flow
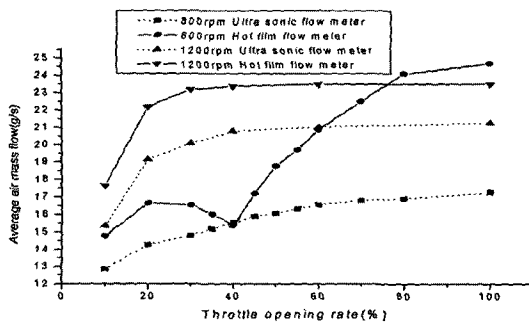(800 rpm, WOT)

Fig. 5 Comparison of air mass flow
(1200 rpm, WOT)

Fig. 6 Air mass flow vs. throttle openting rate

with HFM and USFM. Engine operating condition is 800 rpm and 1200 rpm, WOT. In the case of 800 rpm, the measurement errors start to increase and reach maximum value as throttle opening rate between 40% to WOT because of increment of reverse flow. Before the reverse flow occurs, the HFM has a little error because the HFM can not keep up with flow oscillation. In the case of 1200 rpm, although there is no reverse flow but the HFM has a little error due to the slow response time. This means that the reverse flow and flow oscillation in the intake system has influence on the HFM's error.

Figure 7 explains the measurement error factors with flow fluctuation and reverse flow phenomena at 900 rpm.

Figure 8 shows the average pressure at the surge tank and HFM upstream. Surge tank pressure and HFM upstream pressure are important factors for the reverse flow. As the throttle opening rate increases, the average of surge tank
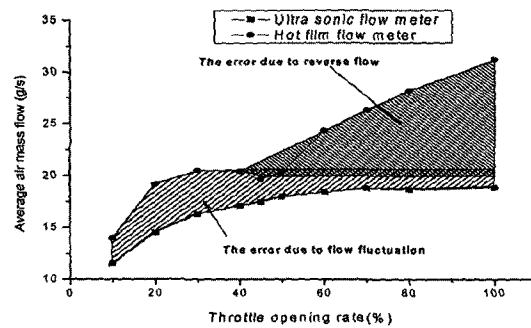

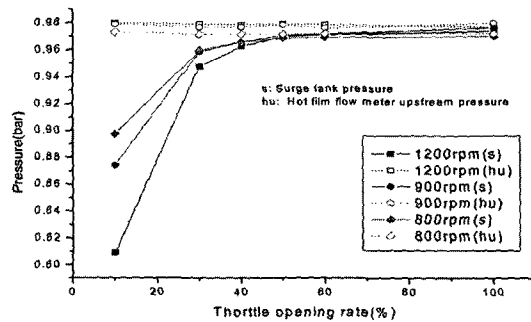**Fig. 7** Measurement error of HFM
(900 rpm, WOT)

Fig. 8 Pressure deviation between surge tank and HFM upstream

pressure gradually increases. If the pressure difference between HFM upstream and the surge tank becomes within 3%, the surge tank pressure is instantaneously higher than the HFM upstream pressure and it causes the reverse flow.

Figures 9 shows air mass flow measured with the HFM and the USFM and the pressure at HFM upstream and the surge tank. In order to find out the relationships between pressure and flow, the pressure curve is shifted by 90 CA (Crank Angle). The surge tank pressure is higher than HFM upstream pressure so air flow direction is from surge tank to air cleaner. Therefore, the generation of reverse flow can be analyzed by pressure gradient of intake system.

Figure 10 represents the reverse flow amounts according to engine speed and throttle opening rate. When the engine speed is 700~900 rpm, the reverse flow increases because the maximum pressure of the surge tank at 900 rpm is higher than that of 800 rpm. The maximum pressure of

the surge tank at 1000 rpm is lower than that of 900 rpm and the reverse flow decreases.

Figure 11 shows the air mass flow measured with HFM and laminar flow meter at various engine speeds. Under 1200 rpm which has reverse flow, HFM has much error. But over 1200 rpm, HFM has also some errors because of flow oscillation in air duct.

In short, the reverse flow only happens with low engine speed and high load operation due to the reversal pressure. And the reverse flow region is in accordance with saturation region at low engine speed.

3.3 Flow characteristics between motoring and firing

The main concern of this study is to investigate on the flow patterns of air duct therefore the engine motoring experiment is compared with engine firing operation.

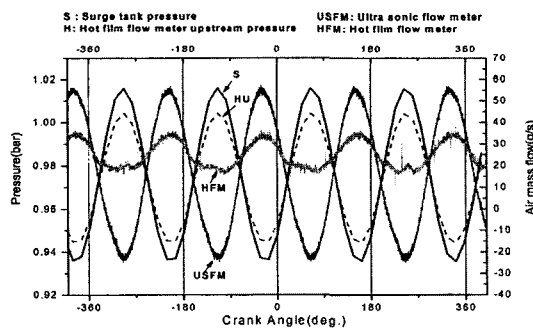Figure 12 shows the comparison of air flow

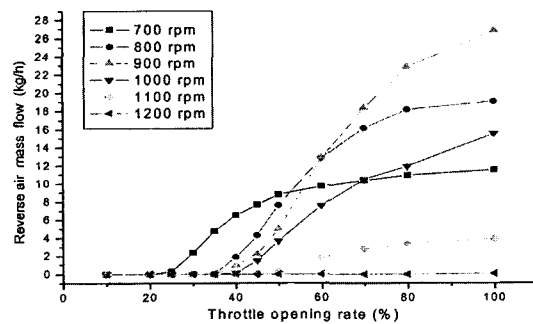**Fig. 9**   Pressure vs. air mass flow
(800 rpm, WOT)

Fig. 11   Averaged air mass flow with engine speed
(WOT)

Fig. 10   Reverse flow according to engine speed and throttle opening rate
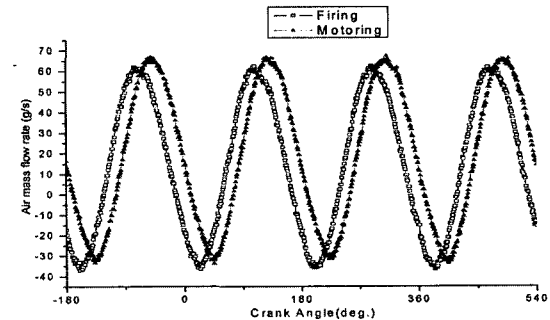

Fig. 12   Comparison of motoring with firing
(900 rpm, WOT)

rate with motoring and firing condition. The average air mass flow rates of firing and motoring are 18.81(g/s) and 23.03(g/s) respectively. The discrepancy of flow rates means that the air mass flow at firing condition decreases due to the lower volumetric efficiency than that of motoring. It is inferred by the pressure difference that the reverse flow between firing and motoring has similar trends.

Figure 13 shows the pressure difference between surge tank and the HFM upstream at 900 rpm, WOT. Compared to motoring operation, the pressure difference of firing has small so the reverse flow increases.

In conclusion, the quantity of the reverse flow of firing is different from that of motoring but the trend is almost the same. Therefore, the motoring experiment has physical meaning for studying flow pattern in the air duct.

3.4 HFM's sensitivity with various intake geometries

3.4.1 Air duct length

Figure 14 shows the air mass flow with USFM according to various air duct length at 1800 rpm, WOT. The air duct length has a little influence on the average air mass flow. However, the duct length has a strong effect on the fluctuation of air flow. In case of air duct length 0.77 m, the amplitude of air flow becomes larger than that of the 1.25 m and 1.73 m.

To confirm the influence of air duct length, the induction system is modeled as an organ
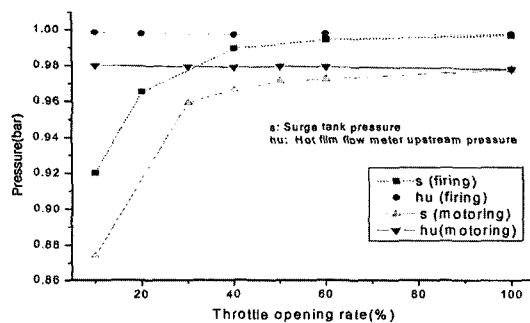
pipe, for which the fundamental resonant frequency (f) of both ends open pipe is given by Eq. 8.

$$f = \frac{nc}{2L}(n=1, 2, 3, \cdots)$$

(8)

c :sound velocity, L :air duct length

In case of air duct length 0.77 m, the of air duct is 167.5 Hz $(n=1)$ by Eq. (8). The air flow frequency at 1800 rpm is 60 Hz. When the f of air duct is divided by air flow frequency, the value is 2.8 and this is close to integer 3. Therefore, the fluctuation of air flow becomes larger due to resonance.

Figure 15 shows the test results of 2400 rpm operation. In case of air duct length 1.73 m, the f of air duct is 86.4 Hz $(n=1)$ and the air duct frequency is 80 Hz. The divided value of above frequencies is almost a unit, so the oscillation of air flow becomes larger than that of 0.77 m and 1.25 m.
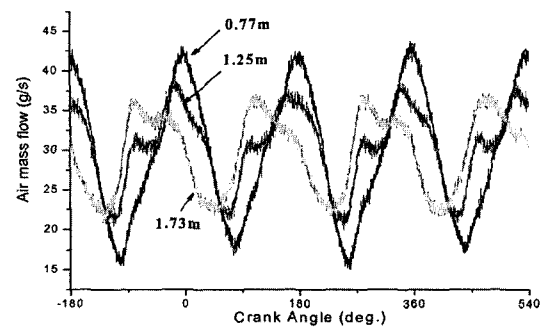

Fig. 14 Air mass flow with various air duct length (USFM, 1800 rpm, WOT, duct angle : 60°)

Fig. 13 Pressure difference between surge tank and HFM upstream (900 rpm, WOT)
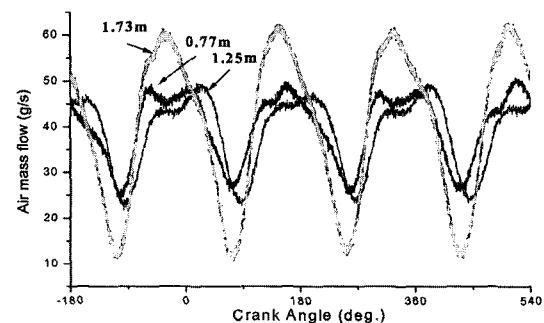

Fig. 15 Air mass flow with various air duct length (USFM, 2400 rpm, WOT, duct angle : 60°)

Figure 16 shows the air mass flow of HFM with various air duct length. The square dot points represent the average air mass flow and the error bars denote the magnitude of flow fluctuation. As air duct length is extended from 0.77 m, the measured amplitude of HFM is reduced.

3.4.2 Air duct angle

Figure 17 shows the air mass flow of USFM with various air duct angle at 900 rpm. The air mass of 0° and 60° cases has similar profile, but in case of 90° angle, average air mass flow and the reverse flow decreases because of the curvature effect. Figure 18 shows the air mass flow with various air duct angle. The average air mass flow of 90° is closer to actual air mass than that of 60° because of small amount of reverse flow.

Though the HFM detects air mass flow, the air duct with 90° layout can not be applicable

to stock engines.

3.4.3 Inserted air duct, inserted air duct round

Figure 19 shows the configuration of inserted duct and round in air cleaner. Figures 20 and 21 show the air mass flow with inserted air duct geometries. From the test results, it is concluded
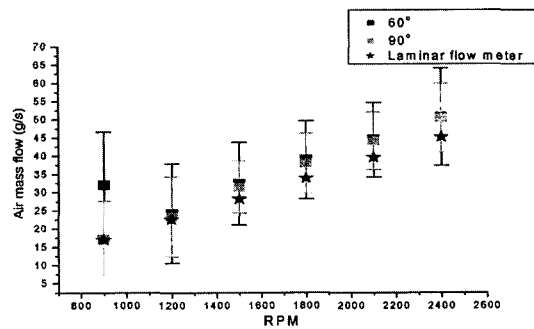

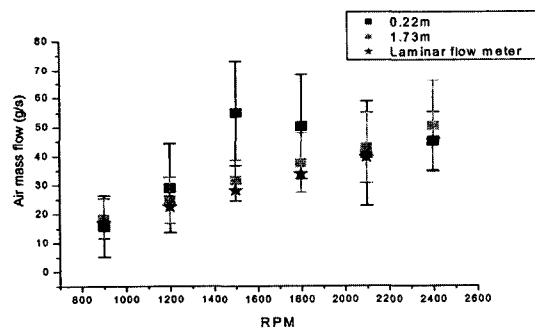**Fig. 18** Air mass flow with various air duct angle (HFM, WOT, air duct length : 0.77 m)

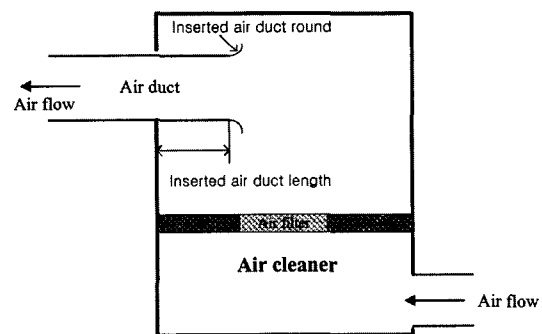**Fig. 16** Air mass flow with various air duct length (HFM, WOT, air duct angle : 60°)

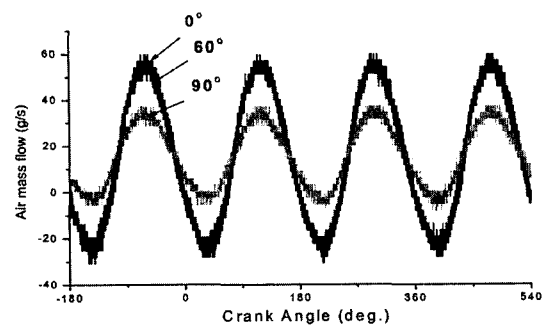**Fig. 19** Schematic diagram of air cleaner (inserted air duct length and round)

Fig. 17 Air mass flow with various air duct angle (USFM, 900 rpm, WOT, air duct length : 0.77 m)
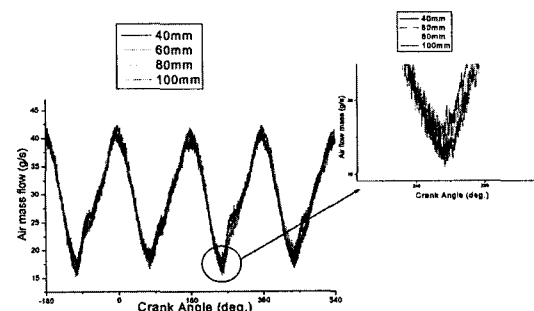

Fig. 20 Air mass flow with inserted air duct length (USFM, 1800 rpm, WOT)
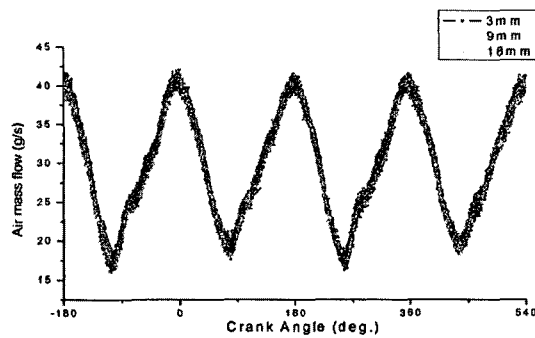
Fig. 21 Air mass flow with inserted air duct round (USFM, 1800 rpm, WOT)

that inserted air duct length and round has little influence on the exact air mass flow of USFM and HFM.

4. Summary

The precise measurement of the intake air flow is the most important factor to control the air fuel ratio of internal combustion engines. The location of intake air flow sensors is the upstream position of throttle body; thus, the analysis of flow pattern in throttle upstream is required for accurate measurement of air flow.

(1) The flow patterns of throttle upstream is grouped by the reverse flow and air flow oscillation, which result in negative instantaneous flow quantity of HFM. Standard air meters are not capable of indicating flow direction. It will produce a air mass flow signal that is much too high when reverse flow occurs.

(2) Generally, the reverse flow originates from low engine speeds and high loads operation. The reverse flow is produced at the saturation throttle opening rate within specific engine speed regions. The reverse flow in the air duct is generated by the reversal pressure gradient between HFM upstream and surge tank. When the average pres-

sure deviation through air duct reaches over 3%, the reverse flow occurs.

(3) As the duct length before HFM increases, the accuracy of HFM is improved because of small amount of flow oscillation.

(4) In the reverse flow region, as the duct angle increases from 0° to 60°, the measurement error of HFM is slightly reduced. However, when the air duct angle approaches to 90°, engine performance is aggravated by flow resistance.

(5) The inserted duct length and round have no significant effect on HFM's sensitivity.

References

Hendricks, E. and Jensen, M., 1990, "Conventional Event Based Engine Control," *SAE paper 900057*.

Heywood, J. B., 1988, "Internal Combustion Engine Fundamentals," McGraw-Hill Company.

Hwang, J. S. and Kauh, S. K., 1997, "Development of a Transit Time Type Dual Path Ultra Sonic Air Flow Meter," *Proceedings of the SAREC 1997*.

Ohata, A. and Ishida, Y., 1982, "Dynamic Inlet Pressure and Volumetric Efficiency of Four Cycle Four Cylinder Engine," *SAE paper 820407*.

Stone, C. R. and Etminan, Y., 1992, "Review of Induction System Design and a Comparison between Prediction and Results from a Single Cylinder Diesel Engine," *SAE paper 921727*.

Sumal, J. S. and Sauer, R., 1984, "Bosch Mass Air Flow Meter : Status and Further Aspects," *SAE paper 840137*.

Svoboda, M. H., 2000, "Comparison of Air Meter Interface Strategies for Engine Management Systems," *SAE paper 2000-01-0546*.

Wave Version 3.6, 2002, "User's Manual," Ricardo.